# Adaption of 2-D look-up tables applied to OCV-curves for aged battery cells

**Anton Klintberg** * **Torsten Wik** *

* *Department of Electrical Engineering, Chalmers University of Technology (email: kanton@chalmers.se, tw@chalmers.se)*

EXTENDED ABSTRACT

In online automotive applications it is common to use look-up tables, or maps, to model nonlinearities in component models that are to be valid over large operating ranges. If the component characteristics change with ageing or wear, these look-up tables must be updated online. For 2-D look-up tables, the existing methods in the literature only adapt the observable parameters in the look-up table, which means that parameters in operating points that have not been visited for a long time may be far from their true values (see e.g. (Hockerdal et al., 2011)).

In this work, correlations between different operating points are used to also update non-observable parameters of the look-up table. The method is applied to Open Circuit Voltage (OCV) curves for aged battery cells. From laboratory experimental data it is demonstrated that the proposed method can significantly reduce the average deviation from an aged OCV-curve compared to keeping the OCV curve from the beginning of the cell's life, both for observable and non-observable parameters.

*Battery cells*

When a battery cell is charging, ions leave the positive electrode and enters the negative electrode in a process called intercalation. At discharge this process is reversed. The energy of a battery cell depends on the difference between the energy states of the lithium intercalated in the positive and in the negative electrode, which give rise to a potential difference. When the cell is at rest, this potential difference is often referred to as the open circuit voltage (OCV).

The remaining capacity of the cell, $Q(t)$, is the energy that can be drawn from the cell until it is fully discharged and the nominal capacity, $Q_{nom}$, is the energy that can be drawn from the cell starting with the cell fully charged and ending with the cell fully discharged. Using these definitions the State of Charge (SoC), can be defined as the ratio of the remaining capacity and the nominal capacity of the cell, i.e.,

$$z_{SoC}(t) = \frac{Q(t)}{Q_{nom}}. \tag{1}$$

The OCV can be measured directly over the terminals of the cell when the cell is at rest. By doing this for different values of SoC, a nonlinear mapping between OCV and SoC is obtained. This mapping is fundamental in equivalent circuit models of battery cells and is usually referred to as the OCV-curve.

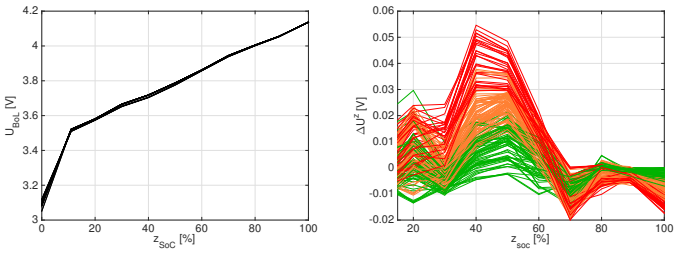


(a) (b)

Fig. 1. (a) Measured OCV-curves from 20 different cells at their beginning of life. (b) Deviation between the measured OCV-curves and the OCV-curves at their beginning of life. Green curves corresponds to $z_{\text{SoH}} \in [90\% \quad 100\%)$, orange curves to $z_{\text{SoH}} \in [80\% \quad 90\%)$ and red curves to $z_{\text{SoH}} \in [70\% \quad 80\%)$. Linear interpolation is used between the measurement points.

Ageing of battery cells is commonly quantified by the so-called State of Health (SoH), which is usually defined as a measure of the capacity fade as the usable capacity of the battery, $Q_{nom}$, decreases with time, i.e.,

$$z_{SoH}(t) = \frac{Q_{nom}(t)}{Q_{nom,BoL}}, \tag{2}$$

where $Q_{nom,BoL}$ is the capacity of the cell at its beginning of life (BoL). As a consequence of ageing the cells' OCV-curves change with time. In Figure 1a OCV-curves measured at BoL of 20 different cells are shown. All the cells should nominally be identical, implying that the OCV-curves are close to identical at BoL. Figure 1b presents the deviations of the measured OCV-curves from their corresponding curves at BoL, each for 10 levels of SoH ranging from 100% down to 70%.

To capture these individual variations we use the following model of an OCV-curve

$$\hat{U}_{OCV}(z_{SoC}, z_{SoH}) = U_{BoL}(z_{SoC}) + \Delta U^z(z_{SoC}, z_{SoH}), \tag{3}$$

where $U_{BoL}$ represents the OCV-curve at the beginning of the cell's life, and $\Delta U^z$ represents the effects of ageing on the OCV-curve.

*2-D Look-up tables*

A look-up table is defined by data values at fixed break-points. Here we denote the break points by $(z_{SoC,i}, z_{SoH,j})$, where $0 \leq z_{SoC,1} \leq \cdots \leq z_{SoC,n} \leq 1$ and $0 \leq z_{SoH,1} \leq \cdots \leq z_{SoH,m} \leq 1$, and consequently $n$ and $m$ defines the size of the table. To keep track of what part of the table that is active we define the time varying indices

$$i(k) = \max\{l_i = 1, ..., n | z_{SoC,l_i} < z_{SoC}(k)\} \quad (4a)$$

$$j(k) = \max\{l_j = 1, ..., m | z_{SoH,l_j} < z_{SoH}(k)\}, \quad (4b)$$

where $k$ denotes the time step. All break points have corresponding data values, $\Delta U_{i,j}$ , which are collected as entries in a concatenated parameter vector

$$\begin{aligned} \Delta U &= [\Delta U_1, \Delta U_2, ..., \Delta U_N]^T \\ &\equiv [\Delta U_{1,1}, ..., \Delta U_{1,m}, \Delta U_{2,1}, ..., \Delta U_{n,m}]^T, \end{aligned} \quad (5)$$

where $N = nm$. Between the break-points the output from the look-up table is described by bilinear interpolation, i.e.

$$\begin{aligned} \Delta U^z =& c_{i,j}\Delta U_{i,j} + c_{i+1,j}\Delta U_{i+1,j} + \\ &+ c_{i,j+1}\Delta U_{i,j+1} + c_{i+1,j+1}\Delta U_{i+1,j+1}, \end{aligned} \quad (6)$$

where

$$c_{i,j} = \frac{(z_{SoH,j+1} - z_{SoH})(z_{SoC,i+1} - z_{SoC})}{(z_{SoH,j+1} - z_{SoH,j})(z_{SoC,i+1} - z_{SoC,i})} \quad (7a)$$

$$c_{i+1,j} = \frac{(z_{SoH,j+1} - z_{SoH})(z_{SoC,i} - z_{SoC})}{(z_{SoH,j+1} - z_{SoH,j})(z_{SoC,i+1} - z_{SoC,i})} \quad (7b)$$

$$c_{i,j+1} = \frac{(z_{SoH} - z_{SoH,j})(z_{SoC,i+1} - z_{SoC})}{(z_{SoH,j+1} - z_{SoH,j})(z_{SoC,i+1} - z_{SoC,i})} \quad (7c)$$

$$c_{i+1,j+1} = \frac{(z_{SoH} - z_{SoH,j})(z_{SoC} - z_{SoC,i})}{(z_{SoH,j+1} - z_{SoH,j})(z_{SoC,i+1} - z_{SoC,i})}. \quad (7d)$$

By introducing $C_k = [c_{1,1}(k), ..., c_{n,m}(k)]$, where all elements not declared in (6) are zero, the look-up table output can be expressed in matrix notation as

$$\Delta U^z(k) = C_k \Delta U(k) + v(k), \quad (8)$$

where $v(k) \sim \mathcal{N}(0, \sigma^2_{v,k})$ naturally is interpreted as measurement noise.

To allow adaption of the unobservable parts (corresponding to the zero entries in $C_k$) of the look-up table we model all table entries as a random walk, i.e.,

$$\Delta U(k+1) = \Delta U(k) + w(k) \quad (9)$$

where $w(k) \sim \mathcal{N}(0, \Sigma_w)$ and white (Fridholm et al., 2016). The covariance should then be set to the symmetric matrix

$$\Sigma_w = \begin{bmatrix} \sigma_1^2 & \rho_{12}\sigma_1\sigma_2 & \cdots & \rho_{1N}\sigma_1\sigma_N \\ \rho_{21}\sigma_2\sigma_1 & \sigma_2^2 & \cdots & \rho_{2N}\sigma_2\sigma_N \\ \vdots & \vdots & \ddots & \vdots \\ \rho_{N1}\sigma_N\sigma_1 & \rho_{N2}\sigma_N\sigma_2 & \cdots & \sigma_N^2 \end{bmatrix}, \quad (10)$$

where $\sigma_i^2$ is the variance for parameter $i$ and $\rho_{ij}$ is the correlation coefficient between parameter $i$ and $j$ given by

$$\rho_{ij} = \frac{\mathbf{E}\Big[\big(\Delta U_i - \mathbf{E}[\Delta U_i]\big)\big(\Delta U_j - \mathbf{E}[\Delta U_j]\big)\Big]}{\sigma_i \sigma_j}. \quad (11)$$

The parameters can then be estimated by applying a Kalman filter to (8) and (9).

*Simulation study*

In this section the potential of the method is demonstrated with a simulation study based on experimental data. In the study the OCV-curves visualized in Figure 1 are randomly divided into two data sets; $\mathcal{D}_I$ comprising data from 10 cells available in the design phase, and $\mathcal{D}_V$ comprising data from 10 cells used for validation. The study aims at investigating how well the algorithm can adapt $\hat{U}_{OCV}$ to the OCV-curves in $\mathcal{D}_V$. However, before the results are presented some more details about the setup need to be explained.

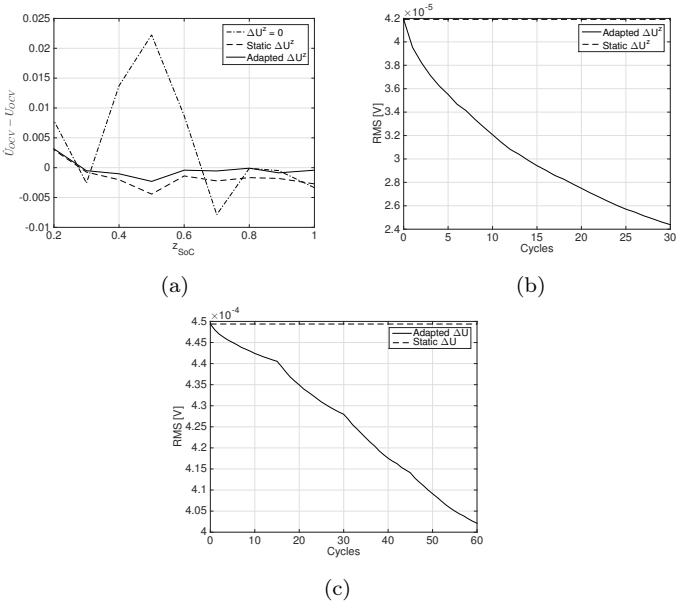


Fig. 2. (a) Deviation from the true OCV-curve for one cell in $\mathcal{D}_V$ for $z_{SoH} = 0.9$. Keeping the OCV-curve at BoL is denoted "$\Delta U^z = 0$" (b) Average RMS for the cells in $\mathcal{D}_V$ calculated for observable parameters with $z_{SoH} = 0.9$. (c) Average RMS for the cells in $\mathcal{D}_V$ calculated for non-observable parameters. The initial guess is denoted "Static $\Delta U^z$" and the output from the algorithm is denoted "Adapted $\Delta U^z$".

This work is not focused on SoH estimation, but it is assumed that we can obtain unbiased estimates, i.e.,

$$\hat{z}_{SoH}(k) = z_{SoH}(k) + v_{SoH}(k), \quad (12)$$

where $v_{SoH}(k) \sim \mathcal{N}(0, \sigma^2_{SoH})$. SoC is estimated by simply integrating the current through the cell. Moreover, the Kalman filter is initiated by parameter values that minimizes the mean square error for the curves in $\mathcal{D}_I$.

In Figure 2a, the deviations from the true OCV-curve for one cell in $\mathcal{D}_V$ are visualised. In the figure it is seen that the adapted OCV-curve is significantly better than keeping the OCV-curve measured at BoL. In Figure 2b the average RMS for all cells in $\mathcal{D}_V$ is presented for each cycle. In the figure we can see that the algorithm, after 30 cycles, manages to reduce the Root Mean Square error (RMS) by more than 40% compared to the initial guess used in the EKF. In Figure 2c we see that the average RMS is reduced with more than 10% even though the RMS is calculated for a region not yet visited. The RMS for keeping the OCV-curve from beginning of life is $15 \cdot 10^{-4}$ V, more than 3.5 times higher than the RMS for the OCV-curves produced by the algorithm.

## REFERENCES


E. Höckerdal, E. Frisk, L. Eriksson, EKF-based adaptation of look-up tables with an air mass-flow sensor application. Journal of Power Sources, vol. 19, p. 442-453, 2011

B. Fridholm, T. Wik, M. Nilsson. Robust recursive impedance estimation for automotive lithium-ion batteries. Journal of Power Sources vol. 304, p. 33-41, 2016